Quantitative dynamic modelling of basin development in the central and eastern North Sea region – coaxial stretching and strain localization

SUSANNE FREDERIKSEN

A new two-dimensional dynamic lithosphere model is used to simulate the Late Palaeozoic to end Danian evolution of the Norwegian-Danish Basin and the post Permian evolution of the Central North Sea including the Central Graben. The transient heat equation and the equations of motion are solved using the finite element method. The lithosphere deforms by brittle and ductile processes through an elasto-visco-plastic rheology depending on temperature, pressure, strain-rate and material parameters. Strain softening dependent on accumulated strain is incorporated. Deposition, erosion and compaction of sediments are simulated. Results show that it is possible to satisfy observations of crustal structure, sediment thickness and surface heat flow for both basins taking all major tectonic and thermal events into consideration. The evolution of the Norwegian-Danish Basin is modelled using a Late Carboniferous – Early Permian thermal event, main rift phase in Early Permian and a minor extensional phase in Triassic. For the Central North Sea two thermal and three tectonic events are simulated: Late Carboniferous – Early Permian and Middle Jurassic thermal events, Early Triassic and Late Jurassic extension, and Late Cretaceous compression. Results show that strain softening may lead to strain localization during extension and therefore may explain observations of upper mantle dipping reflectors in the North Sea. A pure shear dominated extensional regime may change into a simple shear system.

Keywords: dynamic model, extension, strain softening, strain localization, the Norwegian-Danish Basin, the Central North Sea.

Susanne Frederiksen [*sus_fred@hotmail.com*], *Department of Earth Sciences, University of Aarhus, Finlandsgade 8, DK-8200 Århus, Denmark. 15 August 2001.*

Basins are generally formed by one or a combination of three major basin forming mechanisms: stretching, flexure and strike-slip. The present work concerns basins formed by lithospheric stretching. Typical geological and geophysical observations that may be observed in relation to extensional basins are: thinned crust, high surface heat flow, negative Bouguer anomalies, volcanic activity, normal- and listric faults, and rapid tectonic subsidence during extension.

Active and passive rifting are the end-members of the rifting process. Often a rift cannot be classified as being either active or passive but may have aspects of both. In active rifting hot mantle material exerts forces at the base of the lithosphere and thermal convection, uplift and extension are the results. In passive rifting the upwelling of hot mantle material is secondary and the primary thinning is driven by tensional stresses in the lithosphere.

The two end member models of strain geometry are pure shear (McKenzie 1978) and simple shear (Wernicke 1985). In pure shear models no solid body rotations occur. Observations from the Basin and Range Province led to the formulation of a simple shear model (Wernicke 1985). In simple shear extension the majority of strain is accommodated by deformation in a large-scale shear zone cutting through the entire lithosphere.

It can be difficult to determine whether a rift has been formed by pure shear or simple shear deformation (Klemperer & White 1989). As in the case of active versus passive rifting a clear distinction between pure and simple shear can be inappropriate.

In the present work a dynamic thermo-mechanical finite element model has been used to model basin formation and evolution in the Norwegian-Danish Basin (Frederiksen et al. 2001a) and Central North Sea

(Frederiksen et al. 2001b). The models are tested against observations from profiles intersecting the basins in question. Observations consist of present day sediment distribution, crustal structure and surface heat flow. Seismic observations from the North Sea Basin suggests that strain localization has played a role in the development of the basin. Therefore, preliminary investigations on synthetic examples are used to investigate the effect of strain softening on strain localization (Frederiksen & Braun 2001).

Initially, the problems to be solved in the Norwegian-Danish Basin and the Central North Sea are presented. The following sections describe the numerical model, the results, and the conclusions.

The central and eastern North Sea

The motivation for modelling the Norwegian-Danish Basin (NDB) is the timing of basin formation. Until recently the top pre-Zechstein surface in the NDB was believed to mark the transition from pre- to syn-rift sedimentation (Rasmussen 1978, EUGENO-S Working Group 1988). Subsidence curves indicate that the Triassic was a period of extension (Sørensen 1986, Vejbæk 1989, Nielsen & Balling 1990) but the general lack of faults of Triassic age (Vejbæk 1989, 1997) does not support the idea that Triassic was the main rift phase. On the contrary the presence of faults and rotated blocks in the pre-Upper Rotliegendes strata indicates that the main rifting occurred earlier. Therefore, from structural observations an alternative model is proposed (Vejbæk 1997), which suggests that the main rift phase in the Norwegian-Danish Basin occurred in relation to the Permo-Carboniferous thermal event (Ziegler 1990). Thereby, the top pre-Zechstein surface marks a transition from syn- to post-rift sedimentation. This new hypothesis is tested on a 400 km profile crossing the NDB (Fig. 1). Results show that the formation and evolution of the NDB can be explained by thermal doming in Late Carboniferous and Early Permian combined with a main rift phase in Early Permian and a minor rift phase in Triassic (Frederiksen et al. 2001a).

Observations of tectonite and mylonite shear zones exposed at the surface following exhumation (Vissers et al. 1991, 1997) and dipping reflectors in the upper mantle on seismic lines (Klemperer & White 1989, Reston 1990, Braun & Shaw 1998, Nielsen et al. 2000) motivated the research into strain localization caused by strain softening. In the ductile regime grain-size reduction is often observed in relation to strain localization (Kirby 1985). Therefore, strain localization is likely to take place during a transition from dislocation creep to grain-size sensitive creep (Karato et
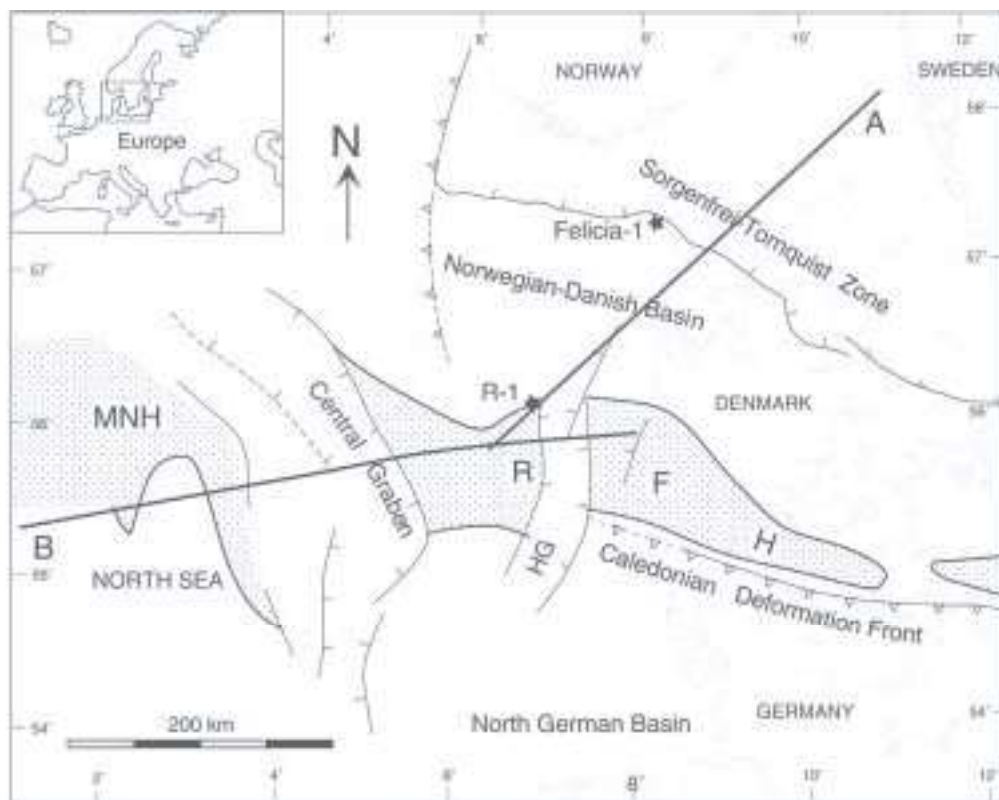

Fig. 1. The position of the modelled profiles crossing the Central Graben (Line B) and the Norwegian-Danish Basin (Line A). RFH: Ringkøbing Fyn High, MNH: Mid North Sea High, HG: Horn Graben.

al. 1986, Handy 1989, Govers & Wortel 1995). A grain-size reduction results in a reduction in material strength for the pressure and temperature conditions characteristic for the uppermost mantle (Handy 1989). A first-order rheological model is used to simulate the transition from 'strong' to 'weak' material. The viscosity of the material is no longer only dependent on strain-rate and temperature but also on accumulated strain. Experiments have been performed in order to investigate the effect of varying the critical strain at which the reduction in strength occurs, the magnitude of the reduction and the strain interval over which the reduction takes place. Results have shown that strain softening can lead to strain localization during extension (Frederiksen & Braun 2001).

The theoretical results achieved using strain softening motivated the consideration of a real data example. Seismic data from MONA LISA Line 3 show dipping reflectors in the upper mantle dipping in opposite directions and showing some symmetry with respect to the deepest part of the Central Graben. It is therefore possible that they have formed during the formation of the Central Graben. An integrated inverse interpretation of seismic refraction data and gravity anomaly data (Nielsen et al. 2000) has provided a detailed crustal model along MONA LISA Line 3. The crustal model shows a distinct local thinning of the crust below the Central Graben. The main fault producing rift phase in the Central North Sea is believed to have occurred in Late Jurassic. Therefore, previous work has concentrated on the Jurassic extensional phase (Sclater & Christie 1980, Wood & Barton 1983, Barton & Wood 1984, Thomsen et al. 1992, Vejbæk 1992). However, they all emphasised that the North Sea rift probably experienced rifting before Jurassic, by some suggested to be in Early Triassic. The aim of the present dynamic model for the Central North Sea is to model the observed crustal structure, sediment thicknesses, surface heat flow and the development of mantle shear zones in relation to extension along a 450 km long profile crossing the Central North Sea (Fig. 1). This is done by a combination of the Permo-Carboniferous thermal event (Ziegler 1990), Early Triassic extension (Sclater & Christie 1980), Middle Jurassic Central North Sea Dome (Underhill & Partington 1993, 1994), Late Jurassic extension (Glennie 1998) and Late Cretaceous inversion (Vejbæk & Andersen 1987, Frederiksen et al. 2001b).

The numerical model

Basin formation and evolution is modelled using a two-dimensional plane-strain lithosphere model. The model comprises a thermal and a mechanical model, where the equations of equilibrium for a continuum and transient heat equation are solved. The models are coupled through the displacements and the temperature field. The temperature affects the viscosity, density and causes thermal stresses in the mechanical model. The lithosphere can deform by elastic, viscous or plastic deformation depending on temperature, pressure, strain rate and material parameters. The finite element method is used to solve the system equations in a mixed frame of reference where the grid mainly follows the material, but flow of material is allowed in the top row of elements in the model.

The thermal model

The two-dimensional Lagrangian transient heat equation reads (Carslaw and Jaeger 1959):

$$\rho c \frac{dT}{dt} = \frac{\partial}{\partial x}\left(\lambda \frac{\partial T}{\partial x}\right) + \frac{\partial}{\partial y}\left(\lambda \frac{\partial T}{\partial y}\right) + A \qquad (1)$$

where ρ is density, c is specific heat, T is temperature, t is time, λ is thermal conductivity, A is radiogenic heat production rate and x and y are spatial coordinates.

The top row of elements in the finite element grid represents the sediments. In order to model erosion and deposition of sediments material must flow across the top row of nodes. This row of nodes therefore becomes Eulerian contrary to the remaining nodes, which are Lagrangian. The Eulerian representation calls for an advective term in the heat equation (Eq. 1), which becomes:

$$\rho c \frac{dT}{dt} = \frac{\partial}{\partial x}\left(\lambda \frac{\partial T}{\partial x}\right) + \frac{\partial}{\partial y}\left(\lambda \frac{\partial T}{\partial y}\right) - \rho c v_y \frac{\partial T}{\partial y} + A \qquad (2)$$

where v_y is the vertical velocity of sediment at the surface.

The boundary conditions for the thermal model are a fixed surface temperature and a spatially and temporally varying background heat flux (Fig. 2). Furthermore, no lateral heat flux is allowed across the two vertical boundaries.
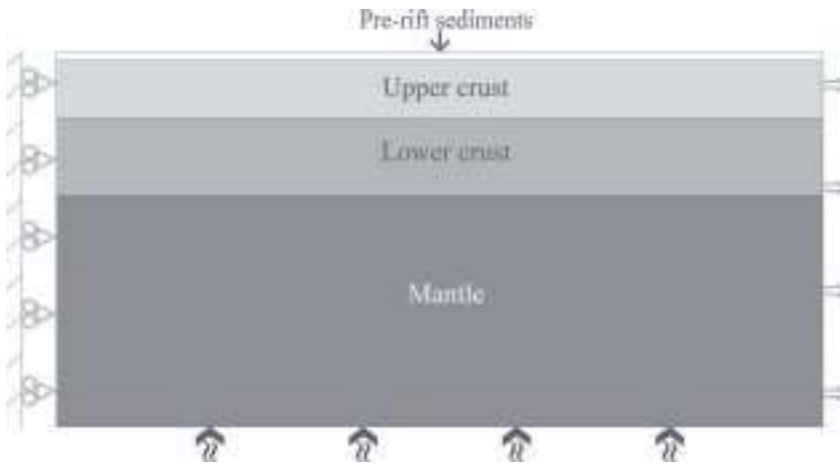
Fig. 2. The initial lithosphere model divided into four different material layers. The left boundary is an axis of symmetry and the right is a no-tilt boundary. The boundary condition at the base of the lithosphere is a spatially varying or constant background heat flux.

The mechanical model

The two-dimensional equations of equilibrium for stress and body forces in a continuum read (Jaeger & Cook 1969):

$$\begin{cases} \dfrac{\partial \sigma_{xx}}{\partial x} + \dfrac{\partial \sigma_{xy}}{\partial y} = 0 \\[2mm] \dfrac{\partial \sigma_{xy}}{\partial x} + \dfrac{\partial \sigma_{yy}}{\partial y} = -\rho g \end{cases} \qquad (3)$$

where σ is the Cauchy stress tensor and g is the acceleration due to gravity.

The stress tensor can be related to strain through the rheological laws. At low deviatoric stress levels the relationship between stress and strain is linear and the material deforms elastically. The generalized Hooke's law reads (Jaeger 1969):

$$\sigma_{ij} = C_{ijkl}\varepsilon_{kl} \qquad i,j,k,l = x,y,z \qquad (4)$$

where ε is the strain tensor and C is a material tensor containing Young's modulus and Poisson's ratio.

At high deviatoric stress levels the lithosphere respond by brittle deformation at low temperature (T) and pressure (p) conditions and by ductile deformation at high p-T conditions. Brittle deformation is modelled using an elasto-plastic rheology where the material deforms elastically when stress is inside the failure envelope and by plastic deformation when stress is on the failure envelope. The failure criterion used is Murrell's extension of Griffith's yield criterion (Jaeger & Cook 1969) given by:

$$F = J_{2D} + 12T_0 p = 0 \qquad (5)$$

where J_{2D} is the second invariant of the deviatoric part of the stress tensor, T_0 is tensile strength and p is pressure.

Ductile deformation is modelled using a non-linear elasto-viscous rheology where the stress-strain relationship can be expressed as (Jaeger & Cook 1969):

$$\dot{\varepsilon}_{ij}^{VE} = C_{ijkl}^{-1}\dot{\sigma}_{kl} + G_{ijkl}\sigma_{kl} \qquad (6)$$

where $\dot{\varepsilon}$ is the strain rate tensor, $\dot{\sigma}$ is the stress rate tensor and G is a tensor containing the viscosity η given by (Braun & Beaumont 1987):

$$\qquad (7)$$

where $\dot{E}_{2D}$ is the second invariant of the strain rate tensor, R is Boltzman's constant and T is temperature. n, B and Q are creep parameters determined in the laboratory for different rocks.

After having incorporated the rheological laws, the stresses in Eq. 3 are expressed in terms of strain. The target in the mechanical part of the model is to find the displacements. Therefore, strain is expressed in terms of displacements. The infinitesimal strain tensor was used for the modelling regarding the Norwegian-Danish Basin and is given by (Jaeger & Cook 1969):

$$\varepsilon_{ij} = \frac{1}{2}\left(\frac{\partial u_i}{\partial x_j} + \frac{\partial u_j}{\partial x_i}\right) \qquad (8)$$

where u is the displacements. In order to handle large deformations and rotations during strain localization a finite strain relationship is required. The mid-point finite strain tensor is very similar to the infinitesimal strain tensor and reads (Braun 1994):

$$\varepsilon_{ij}^{1/2} = \frac{1}{2}\left(\frac{\partial u_i}{\partial x_j^{1/2}} + \frac{\partial u_j}{\partial x_i^{1/2}}\right) \qquad (9)$$

where $x^{1/2}$ are the spatial coordinates of the deformed material in a halfway position between the pre- and post-deformation systems.

Buoyancy forces are incorporated into the model as restoring forces working on density contrast boundaries. The base of the lithosphere, Moho, basement and an internal boundary in the crust are all density contrast boundaries (Fig. 2). Sediment and water are treated as a surface load on basement.

The left vertical boundary is an axis of symmetry and on the right vertical edge of the model kinematic boundary conditions are given.

The sediment model

Basement movements related to extension, isostasy, sea level variations, sediment compaction and thermal expansion or contraction control the accommodation space for the sediments. Two different approaches are used to simulate sediment deposition. In the modelling of the Norwegian-Danish Basin a diffusion equation is used to simulate erosion, lateral sediment transport and deposition of sediments (Frederiksen et al. 2001a):

$$\frac{\partial h}{\partial t} = K_s \nabla^2 h + S \left(h - \Delta SL \right) \qquad (10)$$

where h is the surface topography, $\dfrac{\partial h}{\partial t}$ is rate of change

in topography, K_s is effective diffusivity, S is the source rate and ΔSL is the sea level. The last term in Eq. 10 is a source term used to model sediments from other sources than those related to topography along the profile. The deposition and erosion of sediments are constrained by pre-defined maximum/minimum

sedimentation- and erosion rates. The pre-defined rates are determined from seismic- and well data along the profile (Frederiksen et al. 2001a).

In the second approach the present day sediment thickness observations are used to calculate the exact amount of sediments that should be deposited in each time step. Data are decompacted to surface porosity following the expression given by (Frederiksen et al. 2001b):

$$M = \frac{m + \phi_0 e^{-z/L} \left(e^{-m/L} - 1 \right)}{(1 - \phi_0)} \qquad (11)$$

where M is the thickness of the sediment layer decompacted to surface porosity, m is the present day thickness of the layer, z is present day depth of burial, ϕ_0 is surface porosity and L is a compaction constant. New bulk parameters (density, thermal conductivity, heat production and heat capacity) are calculated for each formation layer at every time step. In the numerical model the layered sediment structure is treated as one layer with bulk properties derived from the layered structure.

Strain softening

A simple *ad hoc* relationship between accumulated strain and viscosity is used to simulate strain softening, which is an effective way of producing strain localization. The softening is performed by reducing the viscosity creep parameter B (Eq. 7) to a new value B^* (Fig. 3) according to (Frederiksen & Braun 2001):

$$B^* = \theta B + \left(1 - \theta\right) B / f \qquad (12)$$

where f is the magnitude of the reduction and θ is a monotonous increasing parameter between 0 and 1 given by:
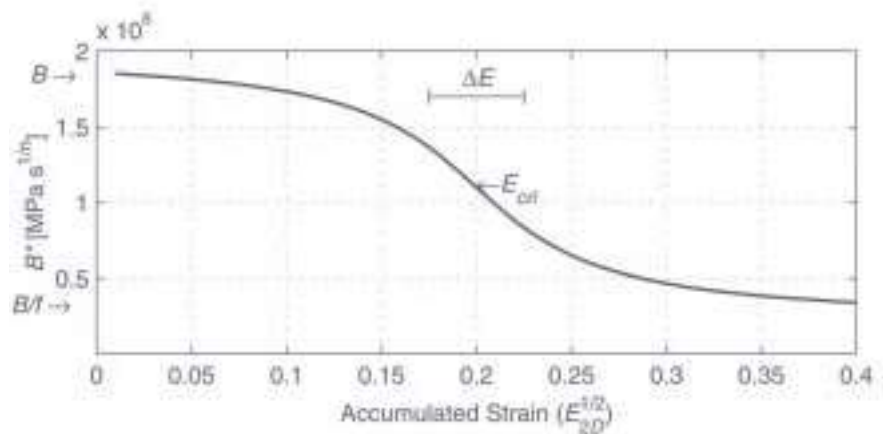

Fig. 3. The arctangent reduction in viscosity is shown as a function of accumulated strain. The three variable parameters describing the function are the critical strain E_{cri} at which the reduction is 50%, the magnitude of the reduction f and the strain interval ΔE over which the reduction occurs (after Frederiksen & Braun 2001).
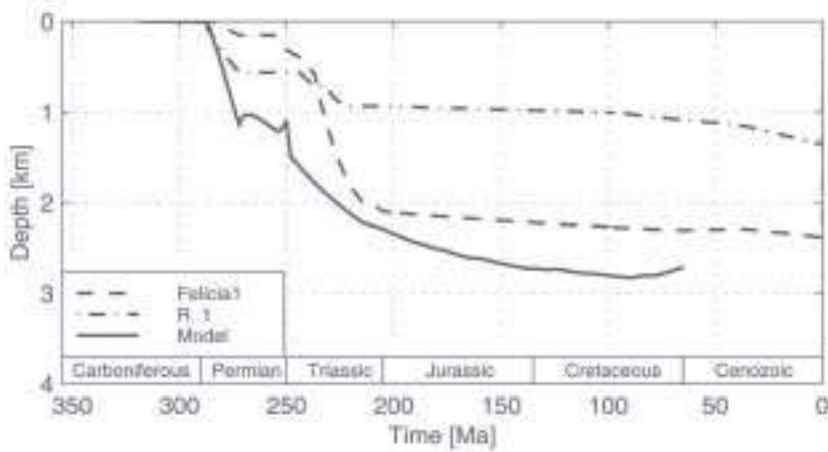
Fig. 4. Tectonic subsidence curves for the wells Felicia-1 and R-1 in the Norwegian-Danish Basin. The full line shows the modelled tectonic subsidence from the centre of the basin. The position of the wells is shown in Fig. 1 (after Frederiksen et al. 2001a).

$$\theta = \frac{1}{2}\left[1 - \frac{2}{\pi}\, atan\left(\frac{E_{2D}^{1/2} - E_{cri}}{\Delta E}\right)\right] \qquad (13)$$

where E_{2D} is the second invariant of the strain tensor and the square root of E_{2D} is a measure of accumulated strain. E_{cri} is the critical strain at which the reduction in viscosity is 50%. ΔE is the strain interval over which the reduction occurs.

Initial model

The initial lithosphere model is divided into four layers: pre-rift sediments, upper crust, lower crust and mantle (Fig. 2). Creep parameters derived from laboratory experiments on wet quartzite are used for the sediments and the upper crust (Paterson & Luan
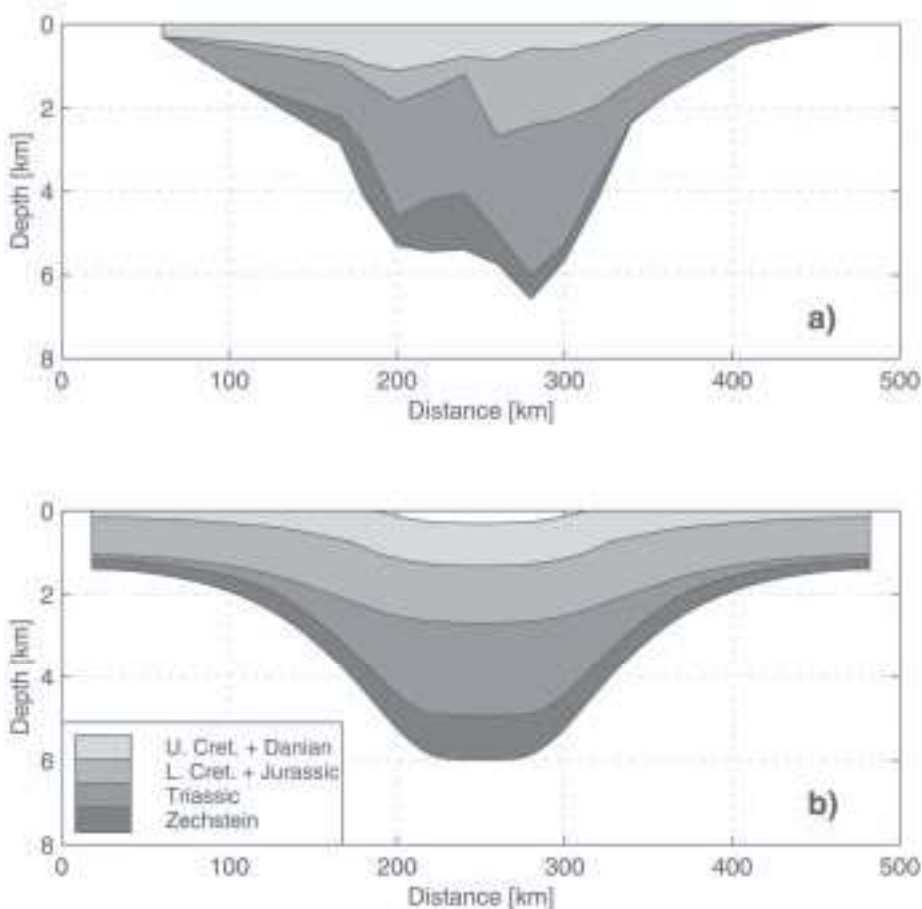

Fig. 5. The observed (a) and modelled (b) sediment distribution at end Danian in the Norwegian-Danish Basin along the chosen profile (Fig. 1) (after Frederiksen et al. 2001a) (25:1).

Fig. 6. The total strain in the lithosphere after 20 % extension. The figure illustrates what happens when the critical strain (E_{cri}) is varied for constant reduction in strength (f = 10) and constant rate of change in strength (ΔE = 0.05). (a) E_{cri} = 0.1, (b) E_{cri} = 0.2 and (c) E_{cri} = 0.3. The thick black lines represent, from top to bottom, the boundaries between sediments/upper crust, upper crust/lower crust, Moho and base of the model (after Frederiksen & Braun 2001).
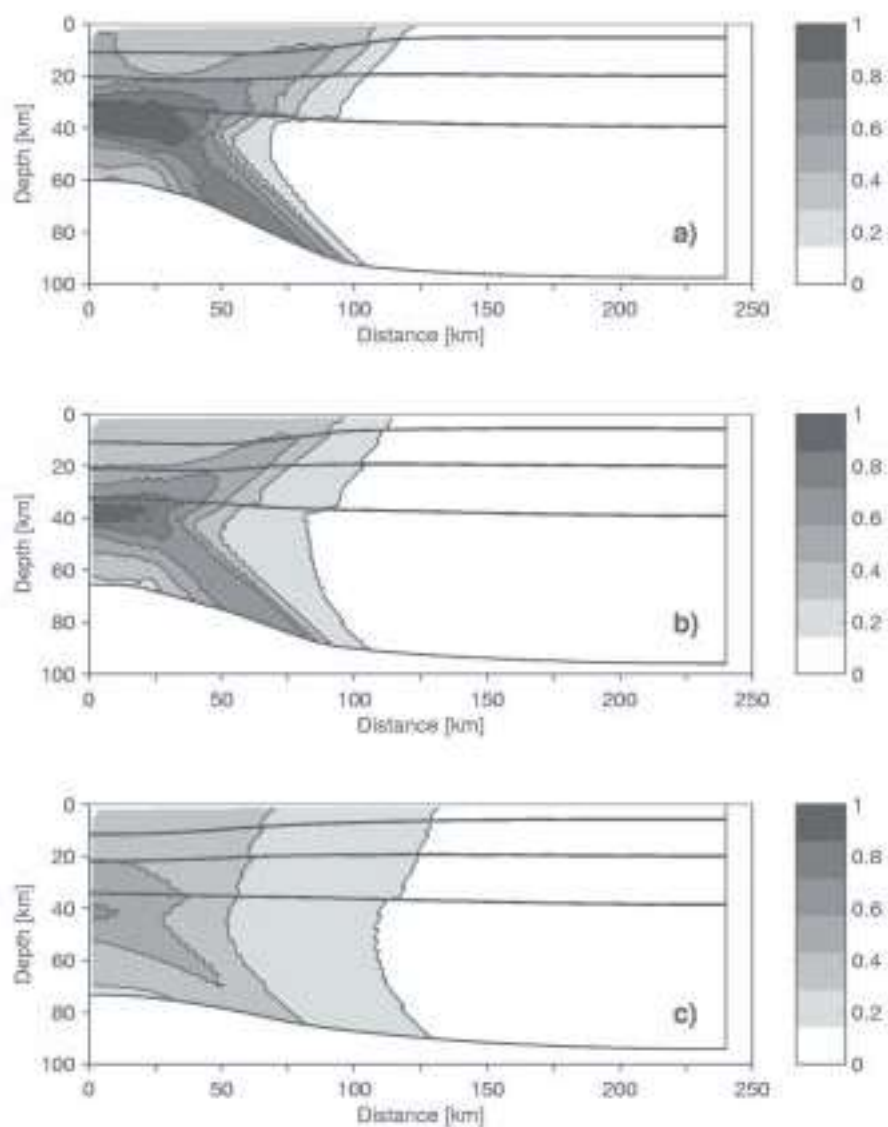
1990). Anorthosite (Shelton & Tullis 1981) and wet dunite (Chopra & Paterson 1981) parameters are used for the lower crust and mantle, respectively.

The thickness and structure of the different layers varies depending on the problem in question. The mechanism for localizing the basin also varies depending on the problem. A thermal basal heat flux anomaly, reduction in tensile strength (T_0 Eq. 5) and a reduction in the creep parameter Q (Eq. 7) has been used (Frederiksen et al. 2001a,b, Frederiksen & Braun 2001).

Modelling results
The Norwegian-Danish Basin

The modelled basin development is initiated with thermal doming and subsequent uplift and erosion of post-rift sediments. The thermal doming simulates the phase of uplift and erosion that is believed to have occurred in Late Carboniferous – Early Permian (Sørensen 1986, Vejbæk 1989, Ziegler 1990). The uplift is modelled by increasing the background heat flux from 30 mW/m² to 60 mW/m² in a zone below the rift in the time interval 320–272 Ma. Observations of
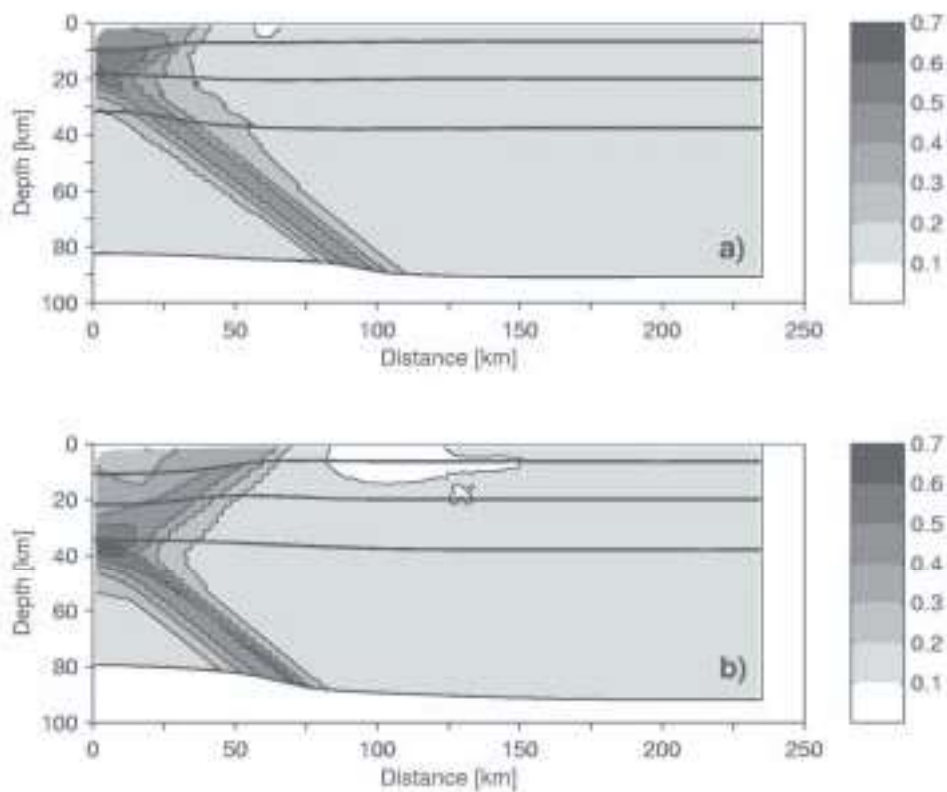
Fig. 7. The distribution of total strain in the lithosphere after 15% of extension. The viscosity reduction parameters are the same in both models ($\Delta E = 0.05$, $E_{cri} = 0.2$, $f = 10$). The difference between the two experiments is width of the zone over which the crustal tensile strength has been reduced by a factor of 2. In (a) the zone is 30 km's broad and 60 km's in (b) (after Frederiksen & Braun 2001).

wrench faulting in Early Permian indicate extension (Ziegler 1990, Vejbæk 1997). Therefore, an extensional phase is superimposed on the thermal event from 290–272 Ma by moving the right boundary of the model (Fig. 2) with a constant velocity of 1 mm/yr. This corresponds to an overall strain rate of 1.6×10^{-16} s^{-1} and 9% (36 km) extension.

After extension has ceased and the background heat flux is reduced to normal at 30 mW/m^2 the lithosphere subsides without deposition of sediments. Thereby, accommodation space is retained and the Rotliegendes units are modelled to have subsided substantially below sea level in accordance with observations of the Zechstein Kupferschiefer (Ziegler 1990). The Zechstein Sea floods the area and halite/evaporites are deposited. Numerical tests showed that the observed rapid subsidence in Triassic (Fig. 4) could not be explained by pure thermal subsidence. Therefore, a weak extensional phase is modelled to have taken place in part of Triassic (250–215 Ma). The right boundary of the lithosphere model is moved with a constant velocity of 0.4 mm/yr (5.8×10^{-17} s^{-1}) resulting in 28 km horizontal extension (6.4%). From Late Triassic (215 Ma) to end Danian (56 Ma) the lithosphere subsides due to thermal contraction, sediment loading and sediment compaction.

Generally the model results are in agreement with data. Figure 5 shows the modelled sediment distribution compared to data. The main differences are at the margins and due to processes that occurred after Triassic and therefore not related to the major basin forming processes. The Middle Jurassic Central North Sea Dome affected the southwestern part of the profile. The inversion of the Sorgenfrei-Tornquist Zone in Late Cretaceous – Early Palaeogene and Cenozoic uplift of Fennoscandia affected the northeastern part. Movements on a local scale such as the Fjerritslev Fault are not modelled. Therefore, the model cannot reproduce the displacement observed at about 240–255 km in Figure 5a.

The crystalline crust is thinned by a factor of 1.5 from an initial thickness of 35 km to 23 km. This is in agreement with observations. Furthermore, a modelled surface heat flow of 65–70 mW/m^2 is in agreement with observations (Balling 1995).

Strain localization

Initially the influence of variations in the parameters (E_{cri}, ΔE and f in Eqs. 12 and 13) describing the strain softening behaviour is investigated. Reference values

for the three parameters are chosen ($E_{cri} = 0.2$, $\Delta E = 0.05$ and $f = 10$) and each of them is varied to test the influence on strain localization. The position of the basin is determined by thermally pre-weakening the lithosphere through an increase in background heat flux. In the first three experiments (Fig. 6) the critical strain value is varied.

All three models are extended 20% in the horizontal direction by moving the right boundary of the model (Fig. 2) with a constant velocity of 20 mm/yr in 2 m.y. (3.2×10^{-15} s^{-1}). The first thing to notice is that strain localization occurs in all three cases. Strain is concentrated in a horizontal layer in the upper mantle right below the rift axis and it propagates into a dipping shear zone. It is interesting that strain initiate in what is often regarded to be the strongest region (upper mantle) of the lithosphere. This may affect the mechanical response of the lithosphere such as flexure and isostasy where the presence of a strong 'fibre' in the upper mantle is important (Braun & Beaumont 1989, Weissel & Karner 1989).

The shear zone gets more diffuse for increasing critical strain. This demonstrates how the degree of strain localization depends on the amount of strain that has occurred after the onset of strain softening. Observing the contour lines in Figure 6 it is clear how there is a discontinuity when crossing Moho. Before the onset of strain localization the lithosphere responds by pure shear deformation and the width of the rift zone is similar in the crust and mantle. When strain localization starts in the mantle the width of the rift remains constant in the mantle but increases in the crust. This results in differential shearing between the crust and upper mantle.

The influence of the strain interval over which the reduction in viscosity occurs was investigated using the same model as above, but with $E_{cri} = 0.2$ and varying the strain interval $\Delta E = 0.03$, 0.09 and 0.13. Results show that the shear zone becomes more diffuse for increasing ΔE. It is apparently necessary with an abrupt drop in viscosity for localization to occur.

Increasing the magnitude of strength reduction by increasing the parameter f results in the opposite effect of increasing the strain interval, ΔE. Again the reference values are used and $f = 10$, 100 and 1000. The lithosphere is stretched by 15% in the horizontal direction. Deformation becomes more localized for increasing magnitude of the reduction parameter indicating that the rate of change in strength determines how localized strain becomes. For high values of f a shear zone develops in the crust. This strongly affects deformation in the rift where a shallowing of the rift axis is observed contrary to an over-deepening of the margins close to the shear zone.

In the above described models a thermal anomaly was used to position the basin at the left side of the model (Fig. 2). Experiments were performed where the pre-weakening was created with a reduction in tensile strength (T_0 in Eq. 5) in the crust. The tensile strength is reduced as a function of horizontal distance following an arctangent function as for the reduction in viscosity. In both models shown in Figure 7 the tensile strength is reduced by 50% over a 10 km broad zone. The reference parameters for the strain softening function are used in both models and the horizontal extension is 17.5%. In Figure 7a the critical distance at which the reduction in tensile strength occurs is 30 km. Clearly the crust is the first area of the lithosphere to reach the strain values for initiation of strain softening. The shear zone thereby originates in the crust and propagates into the mantle. In Figure 7b the critical distance is increased to 60 km and a broader region of the crust is thus pre-weakened. This results in the upper mantle reaching the critical strain value first and localization originates just below Moho. Two shear zones develop propagating into crust and mantle, respectively.

Comparing the results of the above experiments with the case of no strain softening (f equals 1 in Eq. 12) demonstrates the great impact strain localization has on the deformation patterns in the lithosphere. In the pure shear model shown in Figure 8 strain occurs
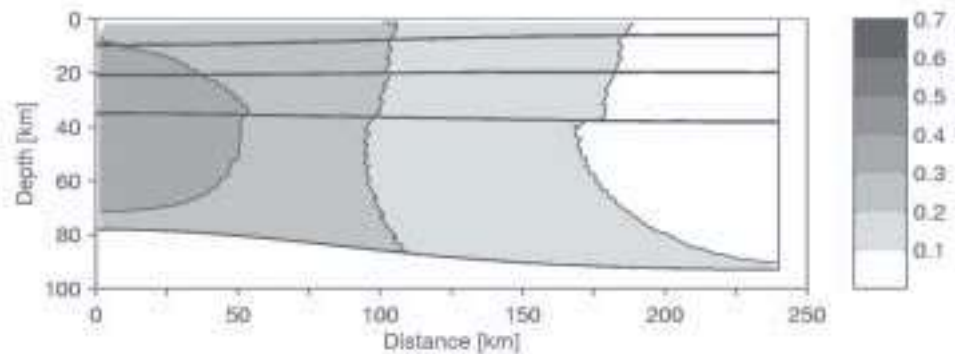

Fig. 8. The distribution of total strain for a pure shear model ($\Delta E = 0.05$, $E_{cri} = 0.2$, $f = 1$) after 20% of extension (after Frederiksen & Braun 2001).
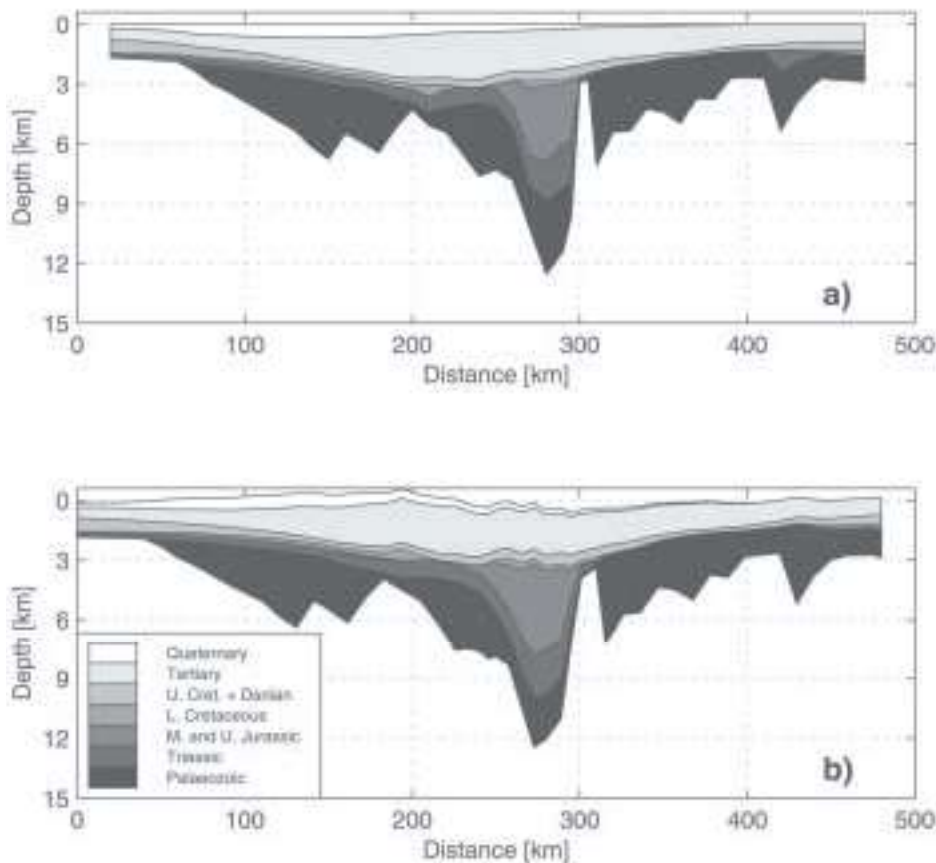
Fig. 9. Observed (a) and modelled (b) present day sediment distribution along the chosen profile (Fig. 1) crossing the Central North Sea (after Frederiksen et al. 2001b) (12:1).

over a broader region of the lithosphere and the basin becomes much broader and shallower.

The Central North Sea

The thermal model is initiated 70 Ma before the mechanical model. This simulates the effects of the Late Carboniferous–Early Permian thermal event (Ziegler 1990) at the onset of extension in Triassic. Information about the pre Permian and Early Permian in the Central Graben is not provided by seismic and well data. Therefore no Early Permian tectonic event is modelled. The background heat flux is increased along the profile with a maximum anomaly of 35 mW/m^2 in the time period 320–272 Ma. The Early Triassic (250–240 Ma) extensional phase (Thomsen et al. 1992, Vejbæk 1992) was simulated by moving the right boundary of the lithosphere model with a constant velocity of 1.7 mm/yr. This corresponds to an overall strain rate of 1.2×10^{-16} s^{-1} and a total horizontal strain of 17 km (3.8%). Following the Triassic extensional phase the lithosphere thermally subsides and sediments are deposited. In Middle Jurassic the entire area is uplifted due to the Central North Sea

Dome (Ziegler 1990). Increasing the background heat flux with a maximum anomaly of 50 mW/m^2 in the time period 180–155 Ma (Underhill & Partington 1993, 1994), simulates the thermal doming. The background heat flux in between the two thermal events is 35 mW/m^2, this is also the heat flux from Middle Jurassic to present day.

The main fault producing event in Late Jurassic (Thomsen et al. 1992, Vejbæk 1992) is simulated by moving the right boundary of the model with a constant velocity of 2 mm/yr (1.36×10^{-16} s^{-1}). The initially 450 km lithosphere profile has been stretched by a total amount of 35 km after the Triassic and Jurassic extensional phases.

Several compressional phases have occurred in Cretaceous and Palaeogene (Vejbæk & Andersen 1987). The compressional events are simulated as one joint phase in the model because of uncertainties in timing and magnitude of each individual event. A velocity of –1.62 mm/yr for a period of 3 Ma is applied at the right boundary to simulate the compressional phase in mid-Maastrichtian (Vejbæk & Andersen 1987). This results in 4.85 km (1%) horizontal shortening of the profile. After the Late Cretaceous compressional phase no further tectonic or thermal events are modelled to have affected the lithosphere.
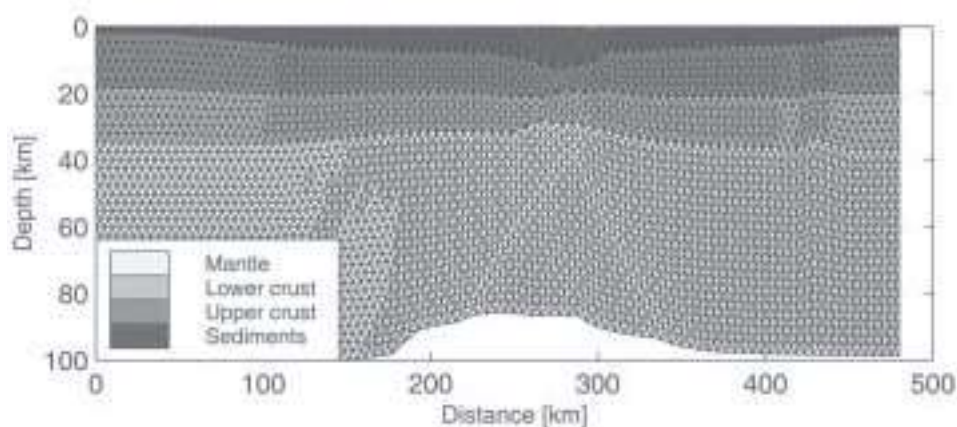
Fig. 10. The distribution of total strain in the Central Graben profile at end Triassic (a) and present day (b) (after Frederiksen et al. 2001b) (2:1).
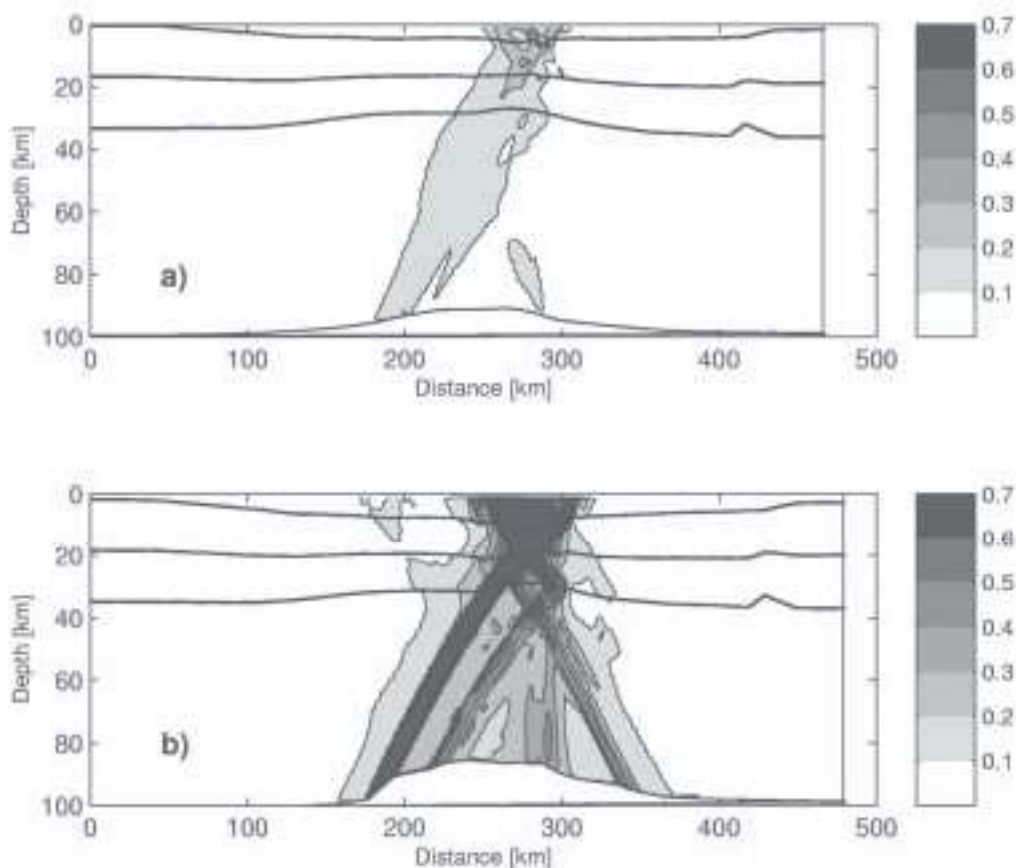
A comparison of the observed and modelled sediment thicknesses along the profile is shown in Figure 9. Generally there is a good agreement between observations and model. Minor discrepancies arise from the large-scale dynamic lithosphere model, which cannot reproduce short wavelength phenomenons, e.g. minor upper crust fault movements. Discrepancies in the present day water depth are observed along the modelled profile. At end Jurassic the entire modelled profile is at sea level. This together with a laterally homogenous Middle Jurassic thermal anomaly results in equal subsidence along the profile. The Cenozoic sediment sequence varies in thickness along the profile and the sequence is thickest west of the graben. The discrepancies indicate that the Central North Sea Dome cannot be modelled as a simple increase in background heat flux with more or less the same anomaly along the profile. Although, a laterally homogenous heat flux anomaly seems justified taking the lateral distribution of the dome into consideration (Underhill & Partington 1993, 1994). Post Jurassic minor thermal pulses may also have affected

Fig. 11. The finite element grid for the Central North Sea model at present day. A distinct thinning of the crust and subsequent elevation of Moho is observed below the Central Graben (after Frederiksen et al. 2001b) (2:1).

the area and resulted in differentiated subsidence along the profile.

Figure 10 shows the distribution of total strain after the Triassic extensional phase (Fig. 10a) and at present day (Fig. 10b). The present day distribution of Triassic sediments indicates that extension occurred over a broad region. Contrary to this the distribution of Jurassic sediments indicates very localized deformation. Therefore, strain softening is not allowed for in Triassic (f equals 1 in Eq. 12), but it is initiated in Jurassic where $E_{cri} = 0.2$, $\Delta E = 0.03$ and $f = 10$. Although an initiation of a shear zone is observed in Figure 10a, a larger region of the lithosphere compared to the Jurassic deformation generally accommodates deformation in Triassic. During the Jurassic extensional phase, strain is concentrated in a west dipping distinct shear zone in combination with two minor shear zones dipping in opposite direction (Fig. 10b).

Modelled local thinning of the crystalline crust below the Central Graben (Fig. 11) is consistent with the crustal model provided by Nielsen et al. (2000). The crust is significantly thinned during the Jurassic extensional phase. The Late Cretaceous compressional phase results in minor thickening of the crust in the Central Graben. The modelled and observed short wavelength Moho structure indicates that the strong 'fibre', which is typically present in the relatively cold olivine rich upper mantle, has been interrupted. The modelled crystalline crust is thinned by a factor 2.1 from an initial thickness of about 33 km to 15.8 km. The modelled present day surface heat flow of 68–71 mW/m^2 in the Central Graben is consistent with data (Balling 1992).

Conclusions

The model can account for the main structural and stratigraphic observations in the Norwegian-Danish Basin. Observations of Rotliegendes volcanism and wrench faulting are simulated by thermal doming in Late Carboniferous to Early Permian combined with extension in Early Permian. This tectonic event led to thinning of the crust and subsidence of the basin. Some accommodation space is preserved during Rotliegendes and the basin has subsided substantially below sea level before transgression of the Zechstein Sea. This period of no or relatively low sedimentation is supported by the presence of the Zechstein Kupferschiefer, which is believed to have been deposited in deep waters. The thick Triassic sedimentary sequence is not easily explained without extension. This is simulated by a relatively long and slow extensional phase, which may explain the general lack of

faults of Triassic age, although some faults are observed in the Sorgenfrei-Tornquist zone. Tectonic events occurring after Triassic such as the Middle Jurassic Central North Sea Dome and inversion in Late Cretaceous – Early Tertiary are not accounted for in the model since the events only affected the basin margins.

A modelled stretching factor of about 1.5, surface heat flow of 65–70 mW/m^2, crystalline crustal thickness of 23 km and sediment stratigraphy are all in good agreement with observations.

Deformation in the Norwegian-Danish Basin was accommodated by pure shear without large deformations and rotations. Indications of simple shear dominated deformation in the Central Graben led to the proposal of a simple first-order rheological law to simulate strain softening. Results have shown that this approach may lead to strain localization if the conditions in the lithosphere are favourable for strain softening to initiate. Increasing the amount of strain occurring after the onset of strain softening leads to a higher degree of strain localization. It also results in shearing between the lower crust and upper mantle that may be imaged by deep reflection profiling. The rate of softening is important for the potential development of shear zones. If the rate is low then the rate of softening and rate of widening of the zone affected by softening is comparable and little or no localization occur. The opposite can be observed for the rate of change in strength. For increasing rate of change in strength a higher degree (narrowing) of localization is observed. For a high rate of change localization occurs in the crust, which results in over-deepening at the flanks and less subsidence at the rift axis.

It has also been shown that strain localization may occur using different pre-weakening mechanisms. A thermal pre-weakening may lead to strain localization and so may a structural weakening such as a reduction of the tensile strength in the crust. In the latter case results showed that the origination of the shear zone is dependent upon the width of the pre-weakened region. For a narrow zone of pre-weakening localization may originate in the crust and propagate into the mantle. A broader zone results in localization originating in the upper mantle just below Moho and two shear zones develop propagating into the crust and mantle, respectively.

The development of shear zones in connection with the main fault producing event in Late Jurassic in the Central Graben has been investigated by using the simple first-order rheological law for strain softening. The main structural and stratigraphic observations in the Central Graben and the development of mantle shear zones in relation to the Late Jurassic extensional phase can be accounted for by the model.

An Early Triassic extensional phase is superimposed on a thermally subsiding lithosphere. The thermal contraction originates from the Late Carboniferous – Early Permian thermal event. The tectonic event results in minor thinning of the crust and initiating strain localization. Thermal doming in Middle Jurassic resulted in doming and erosion of Triassic and Early Jurassic sediments. An extensional phase in Late Jurassic followed the doming event and strain concentrated in the Central Graben and resulted in the deposition of a thick sequence of sediments. In relation to the Jurassic extensional phase strain is localized in one major shear zone and two minor. This is consistent with observations of dipping reflectors in the upper mantle on reflection seismic data from MONA LISA Line 3 (Nielsen et al. 2000). The Late Cretaceous inversion phase results in thickening of the crust in the weak zone below the Central Graben and uplift of the graben. The concentric shape of the dome and the symmetric traces in the erosion of the sediments indicate a simple horizontal thermal event. But the discrepancies in modelled present day water depth may be because the Central North Sea Dome cannot be explained by a simple background heat flux anomaly. Deeper mantle processes may have been at play and the dome may have varied more significantly laterally. Another possibility is minor post Jurassic thermal pulses that resulted in further subsidence.

The narrow thinning of the crust observed below the Central Graben can be simulated by the model and is mainly produced by the Late Jurassic extensional event. The modelled stretching factor of about 2.1 is consistent with observations as is the surface heat flow.

This study has demonstrated the usefulness of two-dimensional dynamic lithosphere models for simulating basin formation and evolution. The model combines lithospheric scale processes with basin scale processes and the impact both of them have on each other. It is possible to satisfy a variety of observations using the same model. A relatively detailed sediment stratigraphy can be modelled on a full-scale lithosphere where effects such as flexure, sediment blanketing and lateral temperature variations are considered. Furthermore, strain localization has successfully been modelled using a simple first-order rheological law for strain softening. Therefore, dipping reflectors in the mantle observed on seismic data in extensional environments may be interpreted as mantle shear zones, and observations of short wavelength Moho structures indicate that the generally strong 'fibre' in the mantle have been interrupted, which may be caused by the development of shear zones.

Acknowledgements

References

Balling, N. 1992: Denmark. In Hurtig, E., Cermák, V., Haenel R. & Zui, V. (Eds) Geothermal Atlas of Europe, pp. 25–28. Haack, Gotha.

Balling, N. 1995: Heat flow and thermal structure of the lithosphere across the Baltic Shield and northern Tornquist Zone. Tectonophysics 244, 13–50.

Barton, P. & Wood, R. 1984: Tectonic evolution of the North Sea basin: crustal stretching and subsidence. Geophysical Journal. Royal Astronomical Society 79, 987–1022.

Braun, J. 1994: Three-dimensional numerical simulations of crustal-scale wrenching using a non-linear failure criterion. Journal of Structural Geology 16, 393–401.

Braun, J. & Beaumont, C. 1987: Styles of continental rifting: Results from dynamic models of lithospheric extension. In Beaumont, C. & Tankard, A.J. (eds) Sedimentary Basins and Basin-forming Mechanisms. Canadian Society Petroleum Geologists, mem. 12, 241–258.

Braun, J. & Beaumont, C. 1989: A physical explanation of the relation between flank uplifts and the breakup unconformity at rifted continental margins. Geology 17, 760–764.

Braun, J. & Shaw, R. 1998: Extension in the Fitzroy Trough, Western Australia: an example of reactivation tectonics. In Braun, J., Dooley, J., Goleby, B., van der Hilst, R. & Klootwijk, C. (eds) The Structure and Evolution of the Australian Lithosphere, AGU Geodynamics Monograph 26, 157–174.

Carslaw, H.S. & Jaeger, J.C. 1959: Conduction of Heat in Solids. 510 pp. Oxford: Oxford University Press.

Chopra, P.N. & Paterson, M.S., 1981: The experimental deformation of dunite. Tectonophysics 78, 453–473.

EUGENO-S Working Group 1988: Crustal structure and tectonic evolution of the transition between the Baltic Shield and the North German Caledonides. Tectonophysics 150, 253–348.

Frederiksen, S. & Braun, J. 2001: Numerical modelling of strain

localization during extension of the continental lithosphere. Earth and Planetary Science Letters 188, 241–251.

Frederiksen, S., Nielsen, S.B. & Balling, N. 2001a: A numerical dynamic model for the Norwegian-Danish Basin. Tectonophysics 343, 165–183.

Frederiksen, S., Nielsen, S.B. & Balling, N. 2001b: Post Permian evolution of the Central North Sea: a numerical model. Tectonophysics 343, 185–203.

Glennie, K.W. 1998: Petroleum Geology of the North Sea: Basic Concepts and Recent Advances & Petroleum Geology. Oxford: Blackwell Science, 376–462.

Govers, R. & Wortel, M.J.R. 1995: Extension of stable continental lithosphere and the initiation of lithopsheric scale faults. Tectonics 14, 1041–1055.

Handy, M.R. 1989: Deformation regimes and the rheological evolution of fault zones in the lithopshere: the effects of pressure, temperature, grainsize and time. Tectonophysics 163, 119–152.

Jaeger, J.C. 1969: Elasticity, Fracture and Flow: with Engineering and Geological Applications. Third edition. 268 pp. London: Methuen and Co. Ltd.

Jaeger, J.C. & Cook, N.G.W. 1979: Fundamentals of Rock Mechanics. 593 pp. London: Chapman and Hall.

Karato, S.I., Paterson, M.S. & Fitzgerald, J.D. 1986: Rheology of synthetic olivine aggregates: influence of grain size and water. Journal of Geophysical Research 91, 8151–8176.

Kirby, S.H. 1985: Rock mechanics observations pertinent to the rheology of the continental lithosphere and the localization of strain along shear zones. Tectonophysics 119, 1–27.

Klemperer, S.L. & White, N. 1989: Coaxial stretching or lithospheric simple shear in the North Sea? evidence from deep seismic profiling and subsidence. In Tankard, A.J. & Balkwill, H.R. (eds) Extensional Tectonics and Stratigraphy of the North Atlantic margins. AAPG Memoir 46, 511–523.

McKenzie, D. 1978: Some remarks on the development of sedimentary basins. Earth and Planetary Science Letters 40, 25–32.

MONA LISA Working Group 1997a: Closure of the Tornquist sea: Constraints from MONA LISA deep seismic reflection data. Geology 25, 1071–1074.

MONA LISA Working Group 1997b: MONA LISA – deep seismic investigations of the lithosphere in the southeastern North Sea. Tectonophysics 269, 1–19.

Nielsen, S.B. & Balling, N. 1990: Modelling Subsidence, Heat Flow, and Hydrocarbon Generation in Extensional Basins. First Break 8, 23–31.

Nielsen, L., Balling, N., Jacobsen, B.H. & MONA LISA Working Group 2000: Seismic and gravity modelling of crustal structure in the Central Graben, North Sea. Observations along MONA LISA profile 3. Tectonophysics 328, 229–244.

Paterson, M.S. & Luan, F.C. 1990: Quartzite rheology under geological conditions. In Knipe, R.J. & Rutter, E.H. (eds) Deformation Mechanisms, Rheology and Tectonics. Geological Society Special Publication 54, 299–307.

Rasmussen, L.B. 1978: Some geological results from the first five Danish exploration wells in the North Sea. Danmarks Geologiske Undersøgelse III række 42, 46 pp.

Reston, T.J. 1990: Mantle shear zones and the evolution of the northern North Sea basin. Geology 18, 272–275.

Sclater, J.G. & Christie, P.A.F. 1980: Continental stretching: an explanation of the post-mid-Cretaceous subsidence of the Central North Sea basin. Journal of Geophysical Research 85 (B7), 3711–3739.

Shelton, G. & Tullis, J. 1981: Experimental flow laws for crustal rocks. EOS 62, 396.

Sørensen, K. 1986, Danish Basin subsidence by Triassic rifting on a lithosphere cooling background. Nature 319, 660–663.

Thomsen, R.O., Lerche, I. & Korstgård, J.A. 1992: The Danish North Sea: a basin prognosis. In Larsen, R.M., Brekke, H., Larsen, B.T. & Talleraas, E. (eds) Structural and Tectonic Modelling and its Application to Petroleum Geology. NPF special publication 1, 439–455.

Underhill, J.R. & Partington, M.A. 1993: Jurassic thermal doming and deflation in the North Sea: implications of the sequence stratigraphic evidence. In Parker, J.R. (ed.) Petroleum Geology of Northwest Europe: Proceedings of the 4th conference. Geological Society London, 337–346.

Underhill, J.R. & Partington, M.A. 1994: Use of maximum flooding surfaces in determining a regional control on the Intra-Aaelian Mid Cimmerian sequence boundary: implications of North Sea basin development and Exxon's Sea-Level Chart. In Posamentier, H.W. & Wiemer, P.J. (eds) Recent Advances in Siliciclastic Sequence Stratigraphy. AAPG, Memoir 58, 449–484.

Vejbæk, O.V. 1989: Effects of asthenospheric heat flow in basin modelling exemplified with the Danish Basin. Earth Planetary Science Letters 95, 97–114.

Vejbæk, O.V. 1992: Geodynamic modelling of the Danish Central Trough. In Larsen, R.M., Brekke, H., Larsen, B.T. & Talleraas, E. (eds) Structural and Tectonic Modelling and its Application to Petroleum Geology. NPF special publication 1, 1–17.

Vejbæk, O.V. 1997: Dybe strukturer i danske sedimentære bassiner. Geologisk Tidsskrift 4, 1–31 (in Danish).

Vejbæk, O.V. & Andersen, C. 1987: Cretaceous – Early Tertiary inversion tectonism in the Danish Central Trough. Tectonophysics 137, 221–238.

Vissers, R.L.M., Drury, M.R., Hoogerduijn Strating, E.H. & van der Wal, D. 1991: Shear zones in the upper mantle: A case study in an Alpine lherzolite massif. Geology 19, 990–993.

Vissers, R.L.M., Drury, M.R., Newman, J. & Fliervoet, T.F. 1997: Mylonitic deformation in upper mantle peridotites of the North Pyrenean Zone (France): implications for strength and strain localization in the lithosphere. Tectonophysics 279, 303–325.

Weissel, J.K. & Karner, G.D. 1989: Flexural uplift of rift flanks due to mechanical unloading of the lithosphere during extension. Journal of Geophysical Research 94, 13919–13950.

Wernicke, B. 1985: Uniform-sense simple shear of the continental lithosphere. Canadian Journal of Earth Sciences 22, 108–125.

Wood, R. & Barton, P. 1983: Crustal thinning and subsidence in the North Sea. Nature 302, 134–136.

Ziegler, P.A. 1990: Geological Atlas of Western and Central Europe 239 pp. Amsterdam: Elsevier.